Spectral engineering via complex patterns of rounded concave and convex nanoresonators achievable via integrated lithography realized by circularly polarized light

Áron Sipos[*], Emese Tóth[**], Attila Török[**], Olivér Fekete[**], Gábor Szabó[**], Mária Csete[**]

[*]Institute of Biophysics, BRC HAS, 6726 Szeged Temesvári krt. 62 Hungary
[**]Department of Optics and Quantum Electronics, University of Szeged, 6720 Szeged, Dóm tér 9, Hungary, mcsete@physx.u-szeged.hu

ABSTRACT

Comparative study has been performed on the spectral and near-field properties of complex concave and convex nano-object patterns that can be fabricated via interferometric illumination of colloid sphere monolayers (IICSM) by applying circularly polarized light. Rectangular patterns of miniarrays composed of a central nanoring and satellite nanocrescents have been designed. Azimuthal orientation dependent spectral effects of the pattern period, composing nano-object shape and size parameters have been uncovered by re-illuminating the complementary patterns by linearly polarized light.

Keywords: interference lithography, plasmonic spectral engineering, Babinet principle

1 INTRODUCTION

Complex plasmonic structures make it possible to realize spectral engineering. Arrays of convex nanoparticles exhibit localized plasmonic resonances (LSPR) on individual nano-objects and surface lattice resonances (SLR) on their arrays [1]. The optical response of concave patterns is more structured due to Fano modulations originating from coupled LSPR and propagating surface plasmon polariton (SPP) modes [2]. Reach physics opens by applying spherical building blocks in complex structures, such as ring and crescent shaped nano-objects [3]. Convex crescent shaped objects support two types of plasmonic resonances occurring, when the **E**-field oscillates along/perpendicularly to their symmetry axis, which are nominated as U/C resonance [4]. Comparison of analogue C-shaped folded dipole antenna array and patch antenna array proved that in complementary patterns illuminated by complementary beams the reflectance and transmittance are interchanged, according to the Babinet principle [5]. Complex patterns of rounded objects can be used as metamaterials [5], moreover polarization rotation can be realized even in zero-order transmitted light [6]. The integrated lithography we have previously developed based on interferometric illumination of colloid sphere monolayers (IICSM) is capable of fabricating complex patterns composed of rounded nano-objects [7-10].

In present study spectral engineering capabilities of complex patterns that can be fabricated via IICSM by applying circularly polarized light are demonstrated.

2 METHODS

In IICSM mini-arrays composed of a central ring and satellite nano-crescents can be fabricated via illuminating a hexagonal colloid sphere monolayer by two interfering circularly polarized beams. Compared to conventional colloid sphere lithography larger degree of freedom is achievable in plasmonic spectral engineering due to that ten geometrical parameters can be tuned independently (Fig. 1a, b). These are p pattern period, t and h nano-object distance and height, $2R_{ring}$ and d' nanoring and nanocrescent diameter, R_{ring}-r_{ring} ring and d'-s*d'/2 nanocrescent thickness, s= $r_{crescent}/R_{crescent}$ ratio of inner and outer nanocrescent radii, ε and ω nanocrescent opening angle and orientation.

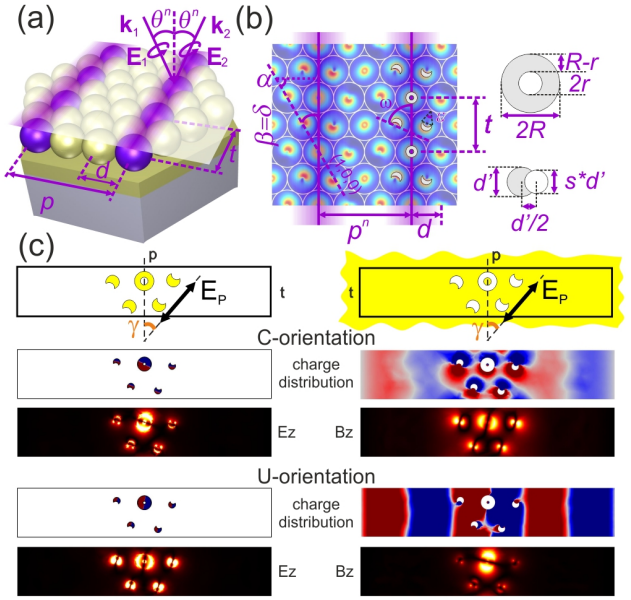

Fig. 1 (a) Realization of IICSM by circularly polarized light, (b) geometrical parameters of resulted concave and convex patterns. (c) Schematics, charge and near-field distribution at global maxima corresponding to a C (top) and U (bottom) resonance on (left) convex and (right) concave p=900 nm periodic pattern in case of s=0.8.

When colloid sphere monolayers are aligned on thin metal films, various rounded shaped nanoholes can be directly fabricated, while a lift-off procedure makes it possible to transfer the nano-objects into analogous convex metal pattern (Fig. 1c).

In present study the original geometrical parameters of the complex patterns were determined based on the near-field distribution, which develops on the substrate under a gold colloid sphere monolayer illuminated by two 400 nm wavelength circularly polarized beams incident in α=60° azimuthal orientation (Fig. 1a).

First complex patterns with three different (p=300 nm, 600 nm, 900 nm) periods that can be generated at θ=41.81°, 19.47°, 12.83° incidence angles and are composed of identical mini-arrays including nanocrescents having s=0.8 parameter, were compared. Detailed studies have been performed on shape and geometrical parameter dependency of 900 nm periodic patterns. First the s parameter influencing the nanocrescent gap size was set to [0.8, 0.9, 11] values (Fig. 2). Than the outer and inner radius of the nanocrescent was multiplied by [0.5, 1, 1.5] factors separately (Fig. 3), finally the outer and inner radius of the nanoring was doubled (Fig. 4).

The concave and convex rectangular patterns were re-illuminated by p-polarized light in complementary azimuthal orientations to demonstrate their spectral engineering capabilities. The transmittance was rectified by subtracting the transmittance of a continuous gold film than this differential signal was normalized to consider the achievement of extraordinary transmission.

3 RESULTS

According to the relative orientation of nanocrescents in the miniarrays, the charge and near-field distributions indicate C/U resonances on the convex (concave) rectangular patterns in γ=106° (16°) / 16° (106°) azimuthal orientations, moreover on the concave patterns localized and propagating plasmonic modes are also observable (Fig 1c, top/bottom in left (right) column).

3.1 Effect of rectangular pattern period

By tuning the pattern periodicity analogous extrema are observable on all complex patterns at visible wavelengths. In C-orientation both of the convex and concave patterns only the FWHM of the peaks modifies (Fig. 2a). On reflectance of the convex miniarray in 106° azimuthal orientation a shoulder develops at 550 nm. The global maximum appears uniformly at 610 nm, which is followed by a local minimum at 640 nm and a slightly smaller local maximum at 660 nm. The local maximum at (900 nm) 770 nm in (p'=600 nm) p''=900 nm pattern is coincident with the Rayleigh anomaly (RA) (λ/n~p' (2λ/n>p")). On the transmittance of the concave miniarray in 16° azimuthal orientation a global minimum develops at 550 nm.

The first local maximum appears again uniformly at 610 nm, which is followed by a local minimum at 630 nm, while the global maximum is observable at 660 nm. The local minimum-maximum at (960-980 nm) 760-780 nm in (p'=600 nm) p''=900 nm pattern is related to RA ((λ_{SPP}~p' and λ/n>p') 2λ_{SPP}~p" and 2λ/n>p").

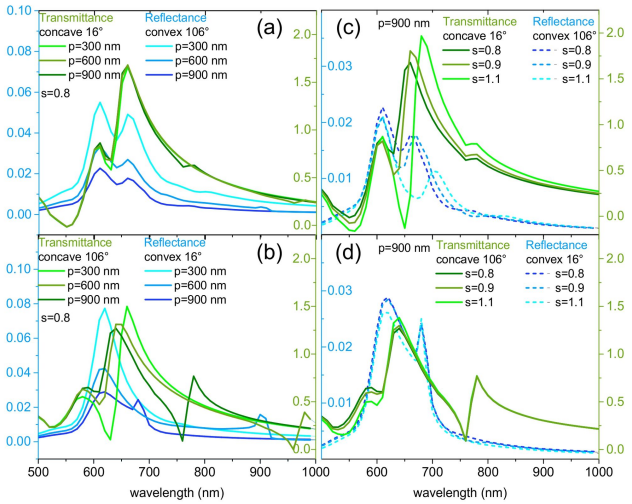

Fig. 2 Effect of (a,b) p pattern periodicity and (c,d) s nanocrescent parameter influencing the gap on spectra in complementary γ azimuthal orientations. (a, c) C-orientation, (b, d) U-orientation.

In contrast, in U-orientation the spectral response corresponding to LSPR is more sensitive to the modification of the periodicity and additional well defined local maxima appear on the patterns caused by RA (Fig. 2b). On the reflectance of the convex miniarray in 16° azimuthal orientation a shoulder develops at 530 nm. The global maximum appears uniformly at 620 nm. The (local maximum at 900 nm) minimum-maximum at 670-680 nm in (p'=600 nm) p"=900 nm pattern is related to RA ((λ/n~p') 2λ/n~p"). The spectral response of the concave pattern is more structured, moreover, on the concave patterns the Fano peaks with their neighboring dips shift noticeably to smaller wavelengths, when the period is increased. Namely, on the transmittance of the concave miniarray in 106° azimuthal orientation a (local) global minimum develops at (520 nm and 530 nm) 520 nm on the (300 nm and 600 nm) 900 nm periodic patterns. The local maximum appears at (580 nm) 590 nm, which is followed by a (global) local minimum at (630 nm and 610 nm) 610 nm, while the global maximum is observable at (660 nm and 640 nm) 640 nm. The local minimum-maximum at (960-980 nm) 760-780 nm in (p'=600 nm) p''=900 nm pattern is related to RA ((λ_{SPP}~p' and λ /n>p') 2λ_{SPP}~p" and 2λ /n>p").

It is important to emphasize that the 900 nm periodic pattern is also capable of resulting in EOT phenomenon despite the large periodicity.

3.2 Effect of nanocrescent *s* parameter

By varying the nanocrescent's gap via *s* parameter tuning causes that the complementary local minimum - local maximum pair on the convex pattern and the local minimum - global maximum pair on the concave patterns slightly shift to larger wavelengths in C-orientation (Fig. 2c). The local minimum gradually deepens on both patterns, the succeeding local maximum on the convex reflectance modifies non-monotonously, while the global maximum on concave transmittance gradually increases. As a result, the optical signal modulation contrast increases on both patterns. The preceding shoulder and global maximum on the convex pattern, as well as the preceding global minimum - local maximum on the concave pattern is almost insensitive to the *s*-parameter.

In contrast, in U-orientation the spectra on either pattern only slightly modify (Fig. 2d). On the convex reflectance only the local modulation appearing after the local maximum shifts to longer wavelength, as the *s*-parameter increases. This indicates that this local modulation is determined by the nano-crescent shape, rather than by the array. On the concave transmittance by increasing the *s*-parameter, the global/local minimum preceding/succeeding the local maximum gradually forward/backward shifts and gradually deepen, as a result the local maximum becomes narrower.

3.3 Effect of nanocrescent outer radius

In C-orientation of the convex pattern the shoulder and the global maximum appears at the same spectral location, while the local minimum as well as the local maximum disappear / shift forward by decreasing / increasing the outer radius of the nanocrescents. In C-orientation of the concave patterns the global minimum appears at the same location. There is a sole maximum in case of smaller outer radius, which is split into a local-global maximum pair with an interleaved local minimum by increasing the $R_{crescent}$. In addition to this a small / huge modulation appears at RA in case of small and intermediate / large $R_{crescent}$ (Fig 3a).

In U-orientation of the convex pattern the shoulder and the first maximum appears at the same location, and the large resonance peak is terminated by a local minimum-maximum pair, which is preceded by an additional interleaved minimum-maximum pair in case of larger outer radius. In U-orientation of the concave patterns the first minimum appears at almost the same location. The local maximum-minimum pair is replaced by an inflection point in case of larger $R_{crescent}$. The global maximum appears at almost the same location, and an additional local minimum appears inside it in case of larger $R_{crescent}$. Large modulation appears in the interval of RA independently of $R_{crescent}$ (Fig 3b).

3.4 Effect of nanocrescent inner radius

By varying the inner radius of nanocrescents in C-orientation of the convex pattern the shoulder slightly modifies. There is only global maximum in case of the smallest inner radius, while the global maximum appears at the same spectral location, and is followed by a local minimum - maximum pair, which shifts forward by increasing the $r_{crescent}$. In C-orientation of the concave patterns the global minimum appears at similar location. There is a sole maximum in case of smaller inner radius, which is split into a local - global maximum pair with an interleaved local minimum. By increasing the $r_{crescent}$ the minimum and global maximum shift forward. In addition to this a slight modulation appears at RA for all inner radii (Fig 3c).

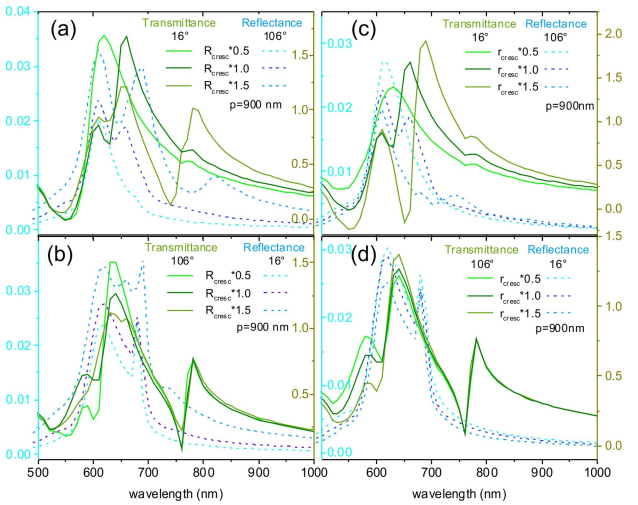

Fig. 3 Effect of (a,b) outer ($R_{crescent}$) and (c,d) inner ($r_{crescent}$) crescent radius on spectra in complementary γ azimuthal orientations. (a, c) C-orientation, (b, d) U-orientation.

In U-orientation of the convex pattern the shoulder and the first maximum appears at the same location, and the large resonance peak is terminated by a local minimum-maximum pair. In U-orientation of the concave patterns the first minimum appears at almost the same location. The local maximum - minimum pair appears also at similar spectral positions, while the global maximum appears at the same location. Large modulation appears in the interval of RA (Fig. 3d).

3.5 Effect of nanoring outer radius

By increasing the outer ring radius of the convex pattern by a factor of two, the shoulder appears at the same location, while only a large global maximum appears instead of the global-local maximum pair in C-orientation. In case of the concave pattern in C-orientation the global minimum appears at the same location, a shoulder and an inflexion point appear instead of the original local maximum-minimum pair, and the succeeding large global maximum slightly shifts forward. Additional local maximum appears beyond RA (Fig 4a).

In case of two-times larger outer ring radius in U-orientation of the convex pattern the shoulder appears at the same location, a local (global) maximum appears instead of a global (local) maximum, which is interleaved by a shoulder instead of the original local minimum, and all corresponding extrema are shifted to larger wavelength. On the concave pattern consisting of a ring with two-times larger outer radius a local-global minimum appears at slightly forward shifted locations instead of the original global-local minimum pair, and the local-global maximum shifts backward-forward. In addition to this a large modulation appears at and beyond RA (Fig. 4b).

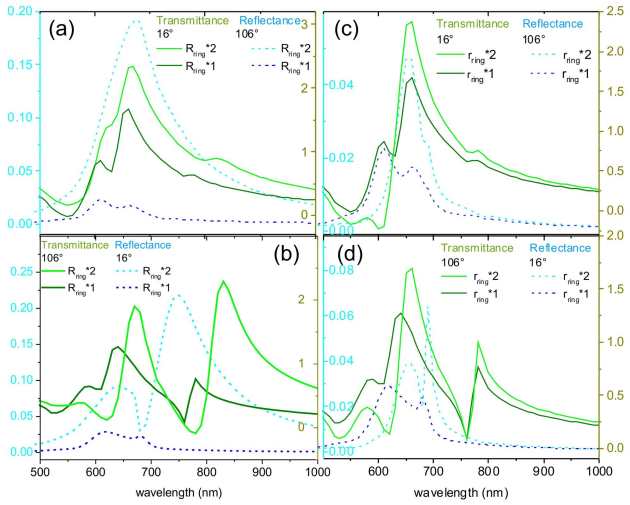

Fig. 4 Effect of (a,b) outer (R_{ring}) and (c, d) inner (r_{ring}) ring radius on spectra in complementary γ azimuthal orientations. (a, c) C-orientation, (b, d) U-orientation.

3.6 Effect of nanoring inner radius

In C-rientation of the convex patterns consisting of a ring with two-times larger inner radius the shoulder slightly modifies, the forward shifted global maximum is followed by inflection points instead of a local minimum-maximum pair, and a slight modulation appears at RA. In C-orientation of the concave pattern consisting of a ring with two-times larger inner radius the local-global minimum appears at the same-backward shifted position, while the local-global maximum is backward shifted-unmodified. Slight modulation appears at RA (Fig. 4c).

In U-orientation of the convex patterns consisting of a ring with two-times larger inner radius the shoulder is forward shifted, the local-global maxima appear at slightly forward shifted locations, with interleaved forward shifted local minimum. In U-orientation of the concave pattern consisting of a ring with two-times larger r_{ring} the global minimum – local maximum pair appear at the same location, while the local minimum – global maximum slightly forward shifts. Large modulation appears at RA (Fig. 4d).

4 CONCLUSIONS

On all inspected patterns the convex reflectance in γ=16°/106° azimuthal orientation corresponds to the concave transmittance in γ=106°/16° azimuthal orientation, and the near-field distributions are also complementary. The results prove that precise plasmonic spectral engineering is realizable via patterns that can be fabricated exclusively via IICSM methodology. The spectral effect is more pronounced in C-orientation, when the *s*-parameter and nanocrescent radii are varied, while the period and ring radii variation results in more well defined modification on the spectra in U-orientation. The complex concave pattern make it possible to achieve EOT phenomenon almost polarization independently. Further studies are in progress to ensure perfect polarization eraser effect in the spectral band of LSPR, or to ensure polarization sensitivity at specific wavelengths by varying the shape and geometrical parameters appropriately.

5 ACKNOWLEDGEMENT

National Research, Development and Innovation Office (NKFIH) “Optimized nanoplasmonics” (K116362); European Union, co-financed by the European Social Fund. “Ultrafast physical processes in atoms, molecules, nanostructures and biological systems” (EFOP-3.6.2-16-2017-00005).

6 REFERENCES

[1] W. Wang, M. Ramezani, A. I. Väkeväinen, P. Törmä, J. G. Rivas and T. W. Odom, Materials Today 21, 303, 2018

[2] B. Luk’yanchuk, N. I, Zhedulev, S. A. Maier, N. J. Halas, P. Nordlander, H. Giessen and C. T. Chong, Nature Materials 9, 707, 2010

[3] A. Aubry, D. Y. Lei, A. I. Fernández-Dominguez, Y. Sonnefraud, S. A. Maier and J. B. Pendry, Nano Letters 10, 2574, 2010

[4] H. Rochholz, N. Bocchio and M. Kreiter, New Journal of Physics 9, 53, 2007

[5] T. Zentgraf, T. P. Meyrath, A. Seidel, S. Kaiser and H. Giessen: Phys. Rev B 76, 033407, 2007

[6] S. Wu, Z. Zhang, Y. Zhang, K. Zhang, L. Zhou, X. Zhang and Y. Zhu, Phys Rev Lett. 110, 207401, 2013

[7] M. Csete, Á. Sipos, A. Szalai and G. Szabó, IEEE Phot J 4/5, 1909, 2012

[8] Á. Sipos, A. Somogyi, G. Szabó and M. Csete, Plasmonics 9, 1207, 2014

[9] Á. Sipos, A. Szalai and M. Csete, Appl Surf Sci 278, 330, 2013.

[10] M. Csete, Á. Sipos and A. Szalai: “Novel lithographic method with the capability of spectrum engineering to create complex microstructures”, WO2013027075A2/3, US 20140226139 A1, US 9291915 B2 (2016).